Borneo Engineering: Jurnal Teknik Sipil
Vol. 10 No. 2. August 2026, pp. 114-129

ISSN 2685-7553
e-**ISSN 2581-1134**

Research Article

Seismic Response and Reinforcement Efficiency of an HDRB-Isolated Reinforced Concrete Lecture Building in Jakarta

Moh Safii Mansur[1], Kohar Yudoprasetyo[1*], Raden Buyung Anugraha Affandhie[1], Ifarrel Rachmanda Hariyanto[1], Yosi Noviari Wibowo[1], Moh Fadhlan Rosyidi[1], and Idqa Filah Reza[2]

[1] Civil Infrastructure Engineering, Institut Teknologi Sepuluh Nopember, Surabaya, Indonesia
[2] Student Civil Infrastructure Engineering, Institut Teknologi Sepuluh Nopember, Surabaya, Indonesia

[*]Corresponding author: kohar.yudo@its.ac.id
DOI. 10.35334/be.v10i2.839

Article History:
Received: 21 June 2026
Revised: 5 August 2026
Accepted: 8 August 2026

Keywords:
Base isolation,
Fixed-base model,
High-damping rubber bearing,
Reinforced concrete building,
Seismic response.

Abstract
This study evaluates the effectiveness of high-damping rubber bearing (HDRB) base isolation in reducing seismic demand and improving structural design efficiency of an 11-story reinforced concrete lecture building on soft soil in Jakarta. A fixed-base model and an HDRB-isolated model were developed in ETABS using response-spectrum analysis based on SNI 1726:2019. The HDRB system was modeled as an isolation layer with lateral flexibility, vertical stiffness, and hysteretic damping behavior. The comparison includes natural period, seismic base shear, interstory drift, lateral restoring force, isolator compressive stress, and reinforcement demand of beams and columns. The results show that HDRB lengthened the fundamental period to 4.758 s in the X-direction and 4.322 s in the Y-direction. This period shift reduced seismic base shear by 46.94% and 33.62% in the X- and Y-directions, respectively, while maintaining interstory drift within allowable limits. The isolator stress check satisfied the allowable compressive stress, with a maximum utilization ratio of 98.01%. Furthermore, HDRB simplified beam reinforcement from 18 to 7 beam types and reduced longitudinal beam reinforcement by 19.3%. These findings indicate that HDRB base isolation improves seismic response and supports more efficient reinforced-concrete design.

Introduction

Indonesia is located in an active seismic region influenced by tectonic-plate interaction and the Pacific Ring of Fire. This condition causes many regions in Indonesia, including Java Island, to have significant seismic hazard that must be considered in building design (Husen et al., 2024). Jakarta, as a metropolitan area, has a high concentration of population, infrastructure, and public-service functions. The expansion of built-up areas in Jakarta also increases the vulnerability of multi-story buildings to earthquake-induced damage, particularly lecture buildings that accommodate many users at the same time (Wibowo et al., 2024).

In conventional seismic design, the fixed-base model assumes that the structure is restrained at its base, so earthquake-induced ground motion is transferred directly to the superstructure. Although this approach is commonly used, it can produce large inertia forces and interstory drift when the building is located in an area with significant seismic demand. Increasing lateral stiffness may reduce drift, but it can also increase the earthquake force that must be resisted by structural elements. Therefore, a design approach is required that not only strengthens structural members but also reduces the seismic energy transmitted to the superstructure.

One relevant technology is seismic isolation, commonly referred to as base isolation. This system inserts isolation devices between the superstructure and the substructure, thereby lengthening the structural period and reducing the seismic energy transmitted to the superstructure (Shahabi et al., 2020). High-Damping Rubber Bearing (HDRB) is an elastomeric isolator with high horizontal flexibility and high energy-dissipation capacity. With these characteristics, HDRB can potentially reduce base shear and interstory drift without excessively increasing the lateral stiffness of the superstructure.

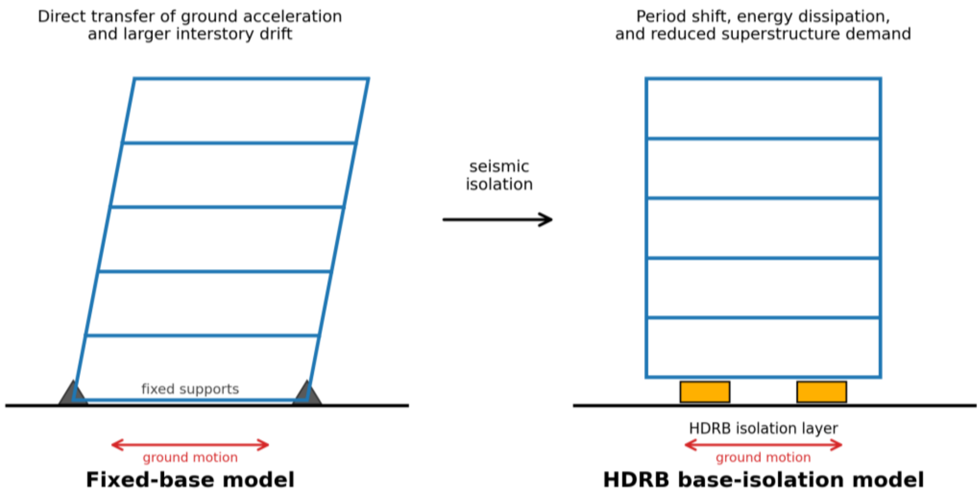

Figure 1. Conceptual comparison between the fixed-base model and the HDRB base-isolation model (Grecia Istiqomah; Herman, Nanang Dalil, 2025; Patel et al., 2024)

Recent studies have shown that base-isolation systems can improve the seismic performance of buildings. Rahardjo et al. (2023) showed that HDRB in a multi-story building on soft soil can reduce base shear and interstory drift. Fakrunnisa and Hayu (2022) compared HDRB and Lead Rubber Bearing (LRB) in an eight-story reinforced-concrete building and reported that HDRB was more effective than LRB in reducing base shear and interstory drift, although it increased structural displacement. Munthe and Iksan (2020) compared isolated-base and non-isolated-base models for the IHF School building in Cimanggis and found that base isolation increased the structural period and reduced base shear and internal forces. Rayendra and Tavio (2024) investigated the effect of HDRB parameters on high-rise buildings in moderate and high seismic regions and emphasized the importance of isolator stiffness and control parameters in structural response. Suwondo et al. (2025) showed that isolator mass, stiffness, and damping ratio affect base shear, natural period, and inelastic story drift. Firmansyah et al. (2025) compared fixed-base and base-isolated reinforced-concrete buildings on soft soil and showed that base isolation can lengthen the period and reduce base shear, acceleration, and drift. Maulida et al. (2025) further demonstrated, using performance-based design, that HDRB installation can reduce base shear and interstory drift and improve the performance level of the structure. In addition, studies on soil-structure interaction in base-isolated buildings indicate that this aspect requires a separate analytical approach; therefore, this study uses the soft-soil site class only for the development of the response spectrum and does not evaluate soil-structure interaction or foundation design (Santoso & Saito, 2024). Recent local studies further support this research direction. Alrasyidi et al. (2026) showed that rubber-bearing isolation can induce a period shift and reduce global inertial response in bridge structures, while Hariyanto et al. (2026) reported that HDRB-based base isolation can substantially reduce base shear and floor acceleration in mid-rise reinforced-concrete buildings. In the context of educational facilities, Yudoprasetyo et al.

(2025) emphasized the importance of numerical structural evaluation and component-level capacity checks to support building safety.

Additional Indonesian studies on structural dynamics and seismic-energy control also support the need to evaluate structural response through period, stiffness, damping, and force-deformation behavior. Hariyanto et al. (2025) showed that shear-wall strengthening combined with vibration-mitigation measures increased the natural frequency of a five-story reinforced-concrete building from 0.66 Hz to 0.855 Hz, indicating that stiffness modification directly affects dynamic response. Hariyanto et al. (2022) further demonstrated, through numerical modeling of a Vertical Shear Link (VSL), that hysteresis curves, deformation modes, and force-displacement response are important indicators for evaluating energy-dissipating structural components.

Although previous studies have confirmed the benefits of base isolation, a focused comparison between the fixed-base model and the HDRB base-isolation model for a multi-story lecture building in Jakarta using SNI 1726:2019 remains limited. The research gap of this study lies in the need for a comparative evaluation that integrates the main seismic-response parameters, namely structural period, seismic base shear, interstory drift control, HDRB lateral restoring-force control, compressive-stress control of the isolators, and the implications for the superstructure response. This study does not merely assess whether HDRB can reduce seismic response; it also evaluates the extent to which the structural behavior becomes more favorable than the fixed-base model in the context of a lecture building in Jakarta. Geotechnical aspects are excluded, except for the use of the soft-soil site class in developing the design response spectrum.

Based on this gap, the research questions addressed in this study are: how the dynamic response differs between the fixed-base model and the HDRB base-isolation model; how HDRB affects the structural period and base shear; how the interstory drift control of the two models compares; whether the HDRB lateral restoring force satisfies the design requirement; whether the compressive stress of each HDRB type remains within the allowable limit; and how HDRB affects the response and efficiency of the superstructure. The objective of this study is to compare the fixed-base method with HDRB base isolation for a lecture building in Jakarta, evaluate the key structural-performance parameters obtained from numerical modeling, and provide a technical basis for using HDRB as an alternative seismic-protection system for multi-story buildings in Jakarta.

Research Method

Structural and Material Data

The structural data used in this study were based on the design data of a lecture building in Jakarta. The building was modeled as a multi-story reinforced-concrete structure located on soft soil. The general structural and material data are presented in Table 1.

Table 1. Structural and material data of the lecture building

Parameter	Data
Building name	Lecture Building
Location	East Jakarta, DKI Jakarta
Number of stories	11 stories, 1 semi-basement, and 1 basement
Building height	52.1 m
Structural material	Reinforced concrete
Structural system	Fixed-base model and HDRB base-isolation model
Site class	Soft soil (SE)
Concrete compressive strength	f'c = 30 MPa and 40 MPa
Steel yield strength	fy = 420 MPa

The applied loads consist of dead load, superimposed dead load, live load, rain load, wind load, and earthquake load. Gravity loads and load combinations refer to SNI 1727:2020 (Badan Standarisasi Nasional, 2020), whereas seismic loading refers to SNI 1726:2019 (Badan Standardisasi Nasional, 2019). A summary of the loading data is presented in Table 2.

Earthquake load and response spectrum. The earthquake load in this study was analyzed using the response spectrum method. The response-spectrum data correspond to the Jakarta location with soft-soil site class SE. Based on the attached spectrum data, the spectral acceleration increases from Sa = 0.266 g at T = 0 s to Sa = 0.664 g at T0 = 0.190 s, and then remains on a plateau until Ts = 0.949 s. After Ts, Sa decreases as the structural period increases. For the HDRB base-isolation model, the effective period of the isolation system is Teff = 3.641 s, so 0.8 Teff occurs at T = 2.913 s with Sa = 0.144 g. This spectrum was used as the seismic input in the X and Y directions in the ETABS model.

Table 2. Loading data used in the analysis

Data type	Description
Dead load	Unit weight of plain concrete 2200 kg/m3 and reinforced concrete 2400 kg/m3.
Superimposed dead load	Cement mortar, half-brick wall, ceiling and frame, ducting/ME, ceramic tiles, roof garden, and gondola.
Live load	Based on SNI 1727:2020 Table 4.3-1.
Rain load	Based on SNI 1727:2020 Section 8.3.
Wind load	Based on SNI 1727:2020 Section 26.1.2.1.
Earthquake load	Based on SNI 1726:2019 using response spectrum analysis.
Load combinations	Based on SNI 1727:2020 and SNI 1726:2019.

The use of an SNI 1726:2019-based response spectrum follows the need for updated seismic-demand evaluation discussed by Hernadi (2019) and Istiono and Lisawiyani (2022). Their findings indicate that changes in seismic-code maps and response-spectrum parameters can influence structural response quantities, particularly base shear and interstory drift, which are also used as the main comparison parameters in this study.

This study does not discuss geotechnical aspects, such as foundation bearing capacity, soil settlement, soil stability, or soil-structure interaction. The soft-soil condition is used only as the site class for determining the seismic-load parameters and the design response spectrum.

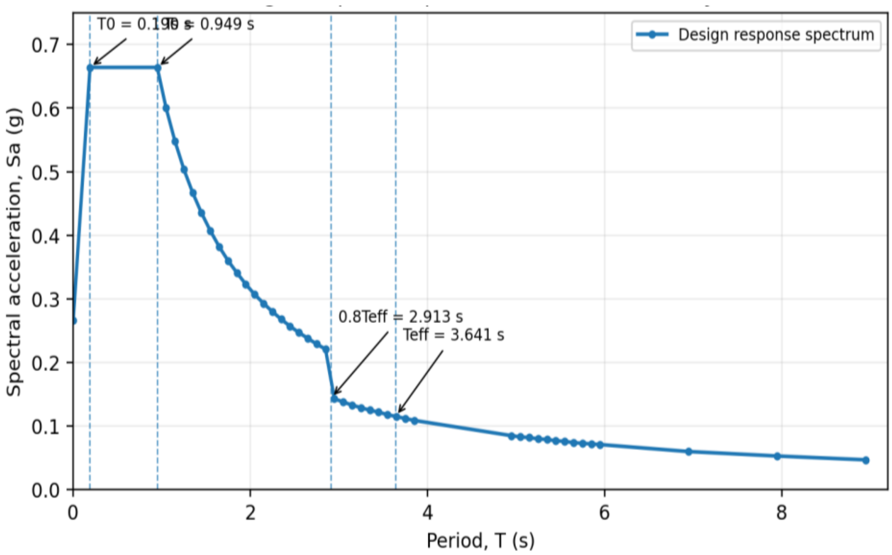

Figure 2. Design response spectrum used in the analysis (Badan Standarisasi Nasional, 2020).

Structural Modeling

Structural modeling was carried out using ETABS. The first model is the fixed-base model, in which the base of the structure is restrained and earthquake-induced ground motion is transferred directly to the superstructure. The second model is the HDRB base-isolation model, in which HDRB devices are installed between the superstructure and the substructure. With this configuration, the superstructure does not fully follow the horizontal ground acceleration because the seismic energy is first dissipated by the isolation layer.

The analysis procedure is described narratively. First, the geometry, material properties, and loads were input into the ETABS model. Second, the fixed-base model was analyzed with restrained base supports. Third, the HDRB base-isolation model was developed by placing isolators at the support points according to the layout plan. Fourth, both models were analyzed using the response spectrum method in accordance with SNI 1726:2019. Fifth, the results were compared in terms of structural period, base shear, interstory drift, lateral restoring force, compressive stress of the isolators, and superstructure response.

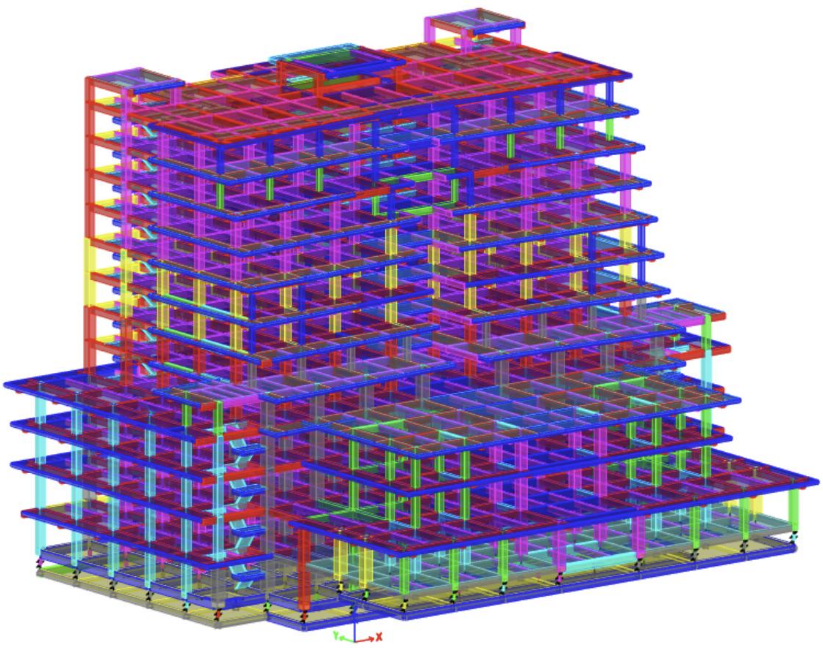

Figure 3. Structural model of the lecture building with HDRB base isolation

Seismic Isolation Concept

Seismic isolation is a structural-protection concept intended to reduce the transfer of earthquake energy from the ground to the superstructure. The system works by inserting isolation elements with relatively low horizontal stiffness and a certain level of damping at the interface between the superstructure and the substructure. In an isolated structure, the first-mode response is generally dominated by deformation in the isolation layer, while the superstructure tends to move approximately as a rigid body. As a result, relative interstory drift and inertia forces in the superstructure can be reduced (Grecia Istiqomah; Herman, Nanang Dalil, 2025).

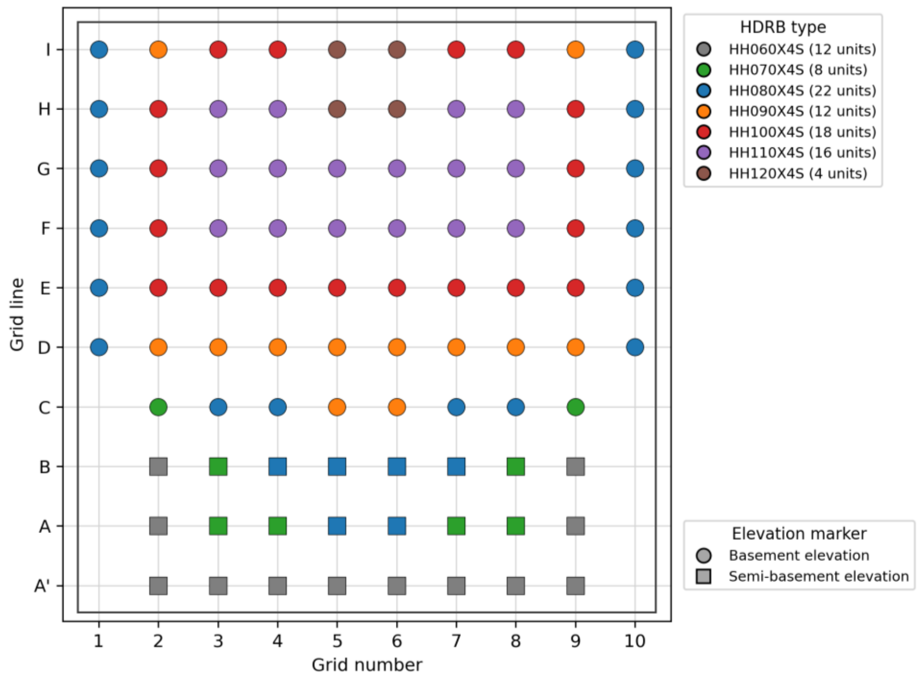

Figure 4. HDRB placement plan by elevation and isolator type

Use of HDRB in the Structure

High-Damping Rubber Bearing (HDRB) is an elastomeric isolator composed of alternating rubber layers and steel plates. Rubber provides horizontal flexibility and energy-dissipation capacity, while the steel plates provide vertical stiffness so that the isolator can support gravity loads. In this study, HDRB was selected as the isolation device for the base-isolation model. The HDRB type used has a shear modulus of 0.392 MPa. This relatively low shear modulus was selected to reduce the lateral stiffness of the isolation system, lengthen the structural period, and reduce the earthquake force transmitted to the superstructure.

The total effective stiffness of the isolation system was obtained by summing the stiffness of each HDRB type multiplied by the number of units used. This value was used to calculate the effective period of the isolation system and the HDRB lateral restoring force. The basic equations used in the analysis are presented as below.

$$K_{\mathrm{eff,total}} = \sum_{i=1}^{m} n_i \, K_{\mathrm{eff},i} \tag{1}$$

$$T_{\mathrm{eff}} = 2\pi \sqrt{\frac{W}{g K_{\mathrm{eff,total}}}} \tag{2}$$

$$F_D = K_{\mathrm{eff,total}} \times \Delta_D \tag{3}$$

$$K_{\mathrm{eff,total}} = 115.568 \text{ kN/mm}, \quad \Delta_D = 360.6 \text{ mm}, \quad F_D = 41{,}673.71 \text{ kN}$$

Based on the isolator data in Table 3, the total effective stiffness of the HDRB system is 115.568 kN/mm. With a total design displacement of 360.599 mm, the lateral restoring force at the design displacement is 41,673.708 kN and is evaluated in next chapter.

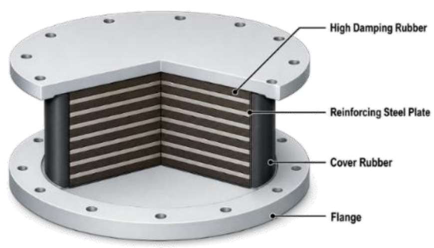

Figure 5. Main components of a High-Damping Rubber Bearing (HDRB) (Bridgestone Corporation, 2010; Grecia Istiqomah; Herman, Nanang Dalil, 2025; Patel et al., 2024)

Table 3. HDRB specifications used in the model (Bridgestone Corporation, 2010)

Parameter	HH060X4S	HH070X4S	HH080X4S	HH090X4S	HH100X4S	HH110X4S	HH120X4S
Diameter (mm)	600	700	800	900	1000	1100	1200
Mass (kg)	660	800	1210	1490	1770	2050	2380
Weight (kN)	6.5	7.9	11.9	14.6	17.3	20.1	23.3
Effective height (mm)	200	202	200	198	201	200	200
Height(mm)	407.9	388.3	422.2	410.8	402.4	400.6	390.2
Allowable vertical load (kN)	1300	2340	4710	7280	10200	12300	14700
Effective stiffness (kN/m)	1700000	2290000	3030000	3870000	4700000	5690000	6780000
Equivalent shear stiffness (kN/m)	554	746	986	1260	1530	1860	2210
Number of units (n)	12	8	22	12	18	16	4

HDRB Material Model for Structural Modeling Input

The HDRB material model was included so that the base-isolation system is not treated merely as a linear spring, but as an isolation element with effective stiffness, equivalent damping, and hysteretic behavior.

Physically, HDRB carries vertical load through alternating rubber layers and steel plates, whereas its horizontal response is governed by rubber shear deformation, restoring force, and energy dissipation. Masaki et al. (2016) showed that the Deformation-History Integral (DHI) model can represent the hysteretic behavior of HDRB over a wide range of shear strains, including HRB(0.4) with a nominal shear modulus of 0.392 MPa and an equivalent damping ratio of approximately 0.22. Park et al. (2023) also showed that HDRB behavior is affected by strain history, the Mullins effect, and hardening at large shear deformation.

In the structural model, HDRB is represented as a nonlinear link element in the horizontal directions and a linear elastic element in the vertical direction. This approach is consistent with the High-Damping Rubber Isolator properties in ETABS/SAP2000/CSiBridge, where bidirectional hysteretic damping is assigned to the shear degrees of freedom, while the axial response is modeled as linear elastic (Computers & Structures, 2025). Oh et al. (2017) reported that HDRB characteristics are influenced by displacement, number of loading cycles, frequency, vertical pressure, temperature, shear-deformation capacity, and vertical stiffness. Therefore, the HDRB material curve used in this study is treated as an initial input idealization and should be validated using manufacturer catalog data or cyclic-test results if the design is extended to nonlinear time-history analysis.

$$\gamma = \frac{\Delta}{t_r} \tag{4}$$

$$\tau = \frac{F}{A} \tag{5}$$

$$K_{eff} = \frac{F_D}{\Delta_D} \tag{6}$$

$$\xi_{eq} = \frac{E_D}{2\pi K_{eff}\delta_D^2} \tag{7}$$

$$F_D = K_{\text{eff,total}} \times \Delta_D \tag{3}$$

The basic material-model relationships are expressed using the shear strain, shear stress, effective stiffness, and equivalent damping ratio of the HDRB system, as shown in Equations (1)–(5). In these equations, Δ is the lateral displacement of the isolator, t_r is the total effective rubber thickness, $F$is the lateral force, $A$is the effective rubber area, E_D is the energy dissipated in one hysteresis cycle, and δ_D is the design displacement. For the preliminary nonlinear-link input, the hysteretic model was developed using the total effective stiffness of the HDRB system of 115.568 kN/mm and the design displacement of 360.599 mm, resulting in a restoring force of 41,673.708 kN.

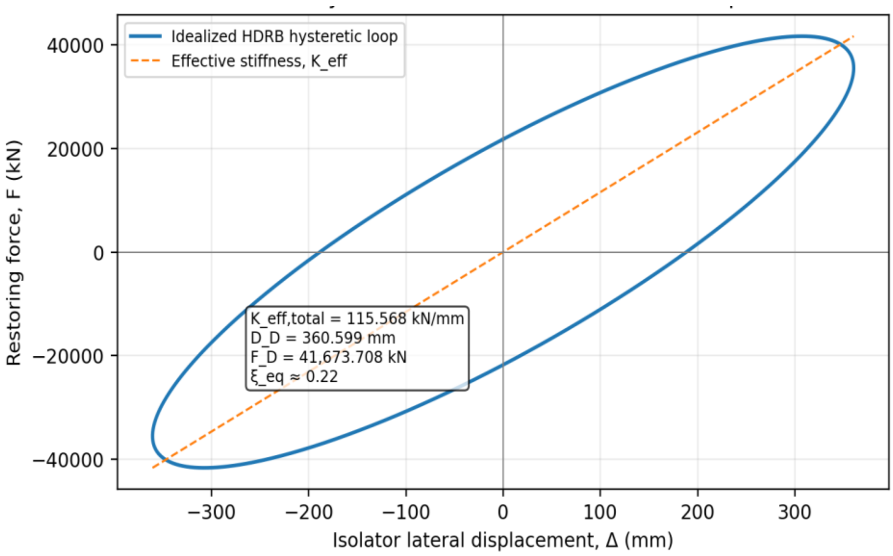

Figure 6. HDRB hysteretic model for structural nonlinear-link input

The HDRB model graph in Figure 6 shows the relationship between lateral restoring force and isolator displacement used as the input reference for the nonlinear link. The dashed line indicates the effective stiffness of the system, while the enclosed hysteretic loop represents the energy dissipated by the high-damping rubber material. With this model, the HDRB base-isolation response is represented not only by the reduction in seismic force but also by the damping mechanism and lateral restoring force that characterize elastomeric isolators.

It should be noted that Figure 6 is an idealized hysteretic model based on study parameters and literature references, not a direct manufacturer test result. In final design, the HDRB link input should be updated using cyclic-shear test curves from the actual HDRB product to calibrate production variability, contact pressure, temperature, aging, and loading-history effects more accurately (Patel et al., 2024).

Results and Discussion

Structural Period Control

The structural period is one of the primary parameters for evaluating the effectiveness of seismic isolation. In the fixed-base model, the fundamental period is 2.425 s in the X direction and 2.285 s in the Y direction. These values indicate that the structure is relatively stiff because its base is assumed to be restrained. In the HDRB base-isolation model, the fundamental period increases to 4.758 s in the X direction and 4.322 s in the Y direction. This increase is consistent with the principle of seismic isolation, in which the structure becomes more flexible at the base level, thereby reducing the acceleration response and earthquake force transmitted to the superstructure.

The period shift observed in this study is consistent with the fundamental behavior of isolated structures reported in previous research. Alrasyidi et al. (2026) found that LRB isolation in an orthotropic highway-bridge system shifted the structural period and reduced global inertial response. Although their study investigated a bridge system and LRB devices, the mechanism is comparable to the HDRB-isolated building model in this study because both systems reduce seismic demand by modifying the dynamic characteristics at the support level. A similar mechanism was also reported by Hariyanto et al. (2026), where base isolation lengthened the structural period as part of a seismic-retrofitting strategy for mid-rise reinforced-concrete buildings.

Table 4. Comparison of structural periods

Parameter	Fixed-base model	HDRB base-isolation model	Description
X-direction period (s)	2.425	4.758	HDRB lengthens the structural period.
Y-direction period (s)	2.285	4.322	HDRB lengthens the structural period.

Seismic Base Shear

Seismic base shear represents the total lateral force that must be resisted by the structural system during an earthquake. Based on the analysis results, the fixed-base model produces base shear values of 18,055.62 kN in the X direction and 18,088.09 kN in the Y direction. After the use of HDRB, the base shear decreases to 9,580.43 kN in the X direction and 12,005.90 kN in the Y direction.

The reduction in base shear in the HDRB model reaches 46.94% in the X direction and 33.63% in the Y direction. This reduction occurs because the isolation system lengthens the structural period and increases the effective damping, thereby reducing the inertia force transmitted to the superstructure. With lower seismic forces, the required capacity of superstructure members can also become more efficient.

Table 5. Comparison of seismic base shear

Seismic direction	Fixed-base base shear (kN)	HDRB base shear (kN)	Reduction (%)
X	18,055.62	9,580.43	46.94
Y	18,088.09	12,005.90	33.63

This result is in line with previous studies that reported force-demand reduction due to isolation systems. Alrasyidi et al. (2026) observed reductions in base shear, internal forces, and bearing reactions after applying LRB isolation to bridge structures. Hariyanto et al. (2026) reported that HDRB-based base isolation could reduce base shear by up to 75.7% in a mid-rise reinforced-concrete building model. The reductions obtained in the present study, namely 46.94% in the X direction and 33.63% in the Y direction, are lower than the upper range reported in some nonlinear studies, but they are reasonable because the level of reduction depends on the site response spectrum, structural mass distribution, isolation stiffness, and equivalent damping adopted in the model.

Interstory Drift Limit Control

Interstory drift limit control was performed to prevent damage to nonstructural components, maintain user comfort, and ensure that the structural performance satisfies SNI 1726:2019. In Figure 7, the X axis represents the interstory drift in millimeters, while the Y axis represents the story level. The drift values are plotted as absolute values so that the fixed-base model and the HDRB base-isolation model can be compared directly in both the X and Y directions.

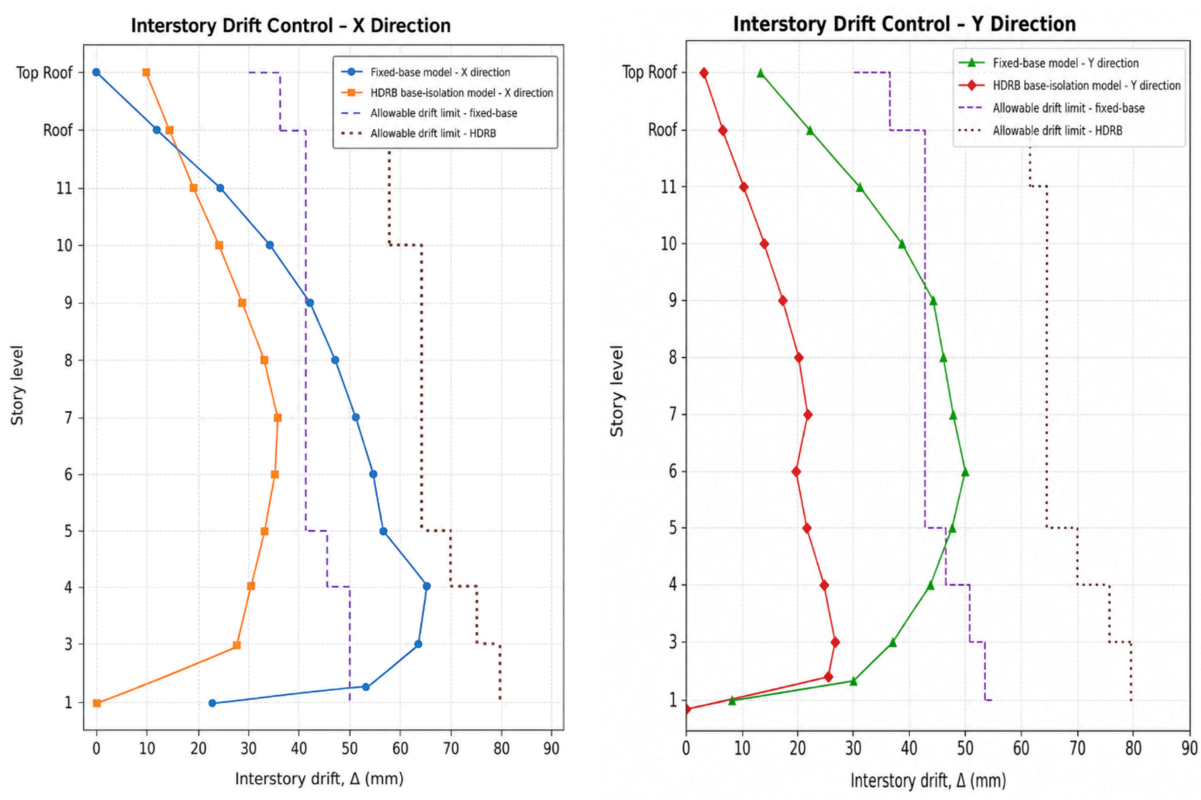

Figure 7. Comparison of interstory drift control in the X and Y directions

In the X direction, the fixed-base model has several stories that exceed the allowable limit, particularly from Story 2 to Story 9. The maximum interstory drift of the fixed-base model in the X direction occurs at Story 4, with a value of 66.05 mm. In contrast, the HDRB base-isolation model remains below the allowable limit at all stories, with a maximum X-direction drift of 55.22 mm at Story 2.

In the Y direction, a similar trend occurs. The fixed-base model has a maximum interstory drift of 60.27 mm at Story 4, and several stories exceed the allowable limit. The HDRB base-isolation model has a maximum Y-direction drift of 29.98 mm at Story 2, and all values remain below the allowable limit. These results indicate that HDRB not only reduces seismic force but also improves the interstory drift distribution, leading to a more controlled superstructure response.

The drift-control trend is also consistent with the structural-control issues discussed in recent study. Istiono and Lisawiyani (2022) highlighted that SNI 1726:2019 can increase structural response demands, including interstory drift, compared with older seismic-code provisions. In this study, the fixed-base model still exceeds the allowable drift limit at several stories, whereas the HDRB model satisfies the limit at all stories. This confirms that the HDRB system reduces the deformation demand on the superstructure by concentrating a larger portion of the lateral displacement in the isolation layer, a behavior also observed in previous HDRB and base-isolation studies (Fakrunnisa & Hayu, 2022; Maulida et al., 2025).

Lateral Restoring-Force Control

Lateral restoring-force control was carried out to ensure that the isolation system is capable of returning the structure toward its original position after earthquake-induced displacement. Based on SNI 1726:2019 Section 12.2.4.4, the isolation system must provide a restoring force that satisfies the minimum requirement with respect to the effective structural weight. The evaluation was carried out using the basic restoring-force equation $F = k_{eff} \, x \, \delta_D$, where k is the total effective stiffness of the isolation system and Delta is the total design displacement.

The calculation shows that the lateral restoring force of the HDRB system is 41,673.708 kN, which is greater than the minimum requirement of $0.025W$ = 9,517.663 kN. Therefore, the isolation system satisfies the lateral restoring-force control and is considered capable of providing an adequate re-centering mechanism after lateral deformation.

This restoring-force verification is important because base-isolated systems may reduce force demand while increasing displacement demand at the isolation level. Hariyanto et al. (2026) noted that base-isolation systems can produce larger lateral displacement than fixed-base conditions, whereas damping systems tend to provide more controlled displacement. Therefore, the restoring-force check in this study is essential to ensure that the HDRB system not only reduces seismic demand but also provides adequate re-centering capacity after lateral deformation.

Table 6. Lateral restoring-force control of the HDRB system

Parameter	Value	Description
Total effective stiffness, k_{eff}	115.568 kN/mm	Sum of the stiffness of all HDRB units.
Total design displacement, δ_D	360.599 mm	Design displacement of the isolation system.
Effective structural weight, W	380,706.55 kN	Effective weight of the structure.
Lateral restoring force, $F = k_{eff} \, x \, \delta_D$	41,673.708 kN	Restoring force at the design displacement.
Minimum requirement, $0.025W$	9,517.663 kN	Minimum restoring-force requirement.
Verification	F >= 0.025W	OK

Compressive-Stress Control of HDRB Base Isolators

Compressive-stress control was performed to ensure that each HDRB unit remains stable in carrying the vertical load when the structure undergoes the design lateral displacement. This check compares the actual compressive stress with the allowable stress for each HDRB type. The actual compressive stress is calculated by dividing the isolator axial force by the effective area, or $\sigma_{act} = P/A_{eff}$.

The control data for each individual isolator point are not presented in full in order to keep the paper concise. Instead, the data are summarized as the critical value for each HDRB type, namely the maximum compressive stress among all isolator points of that type. This presentation allows the adequacy of each isolator type to be evaluated without displaying a long repetitive table.

Table 7. Summary of compressive-stress control for HDRB base isolators

HDRB type	A_{eff} (mm²)	Critica l grid	P_{max} (kN)	$\sigma_{act,max}$ (MPa)	σ_{all} (MPa)	Utilizat ion (%)	Check
HH060X4S	2826	6-A'	747.06	2.64	4.6	57.47	OK
HH070X4S	3847	3-B	2,243.52	5.83	6.1	95.60	OK
HH080X4S	5023	6-C	4,605.81	9.17	9.4	97.55	OK
HH090X4S	6359	2-D	5,583.35	8.78	11.5	76.35	OK
HH100X4S	7849	4-F	10,000.51	12.74	13.0	98.01	OK
HH110X4S	9480	3-H	11,347.75	11.97	13.0	92.08	OK
HH120X4S	11286	6-H	12,365.25	10.96	13.0	84.28	OK

Based on Table 7, all HDRB types satisfy the compressive-stress criterion because the maximum actual stress remains lower than the allowable stress. The most critical condition occurs for type HH100X4S at Grid 4-F, with a maximum axial force of 10,000.51 kN, a compressive stress of 12.74 MPa, and a utilization ratio of 98.01% relative to the allowable stress of 13.0 MPa. Types HH080X4S and

HH070X4S also approach their allowable limits, with utilization ratios of 97.55% and 95.60%, respectively; therefore, both types should receive particular attention during design verification and product-specification checking.

The graph in Figure 8 shows that the utilization ratios of all HDRB types are below 100%. This indicates that the compressive capacity of the isolators satisfies the allowable limit based on the axial forces and effective areas used in the analysis. Therefore, from the compressive-stress perspective, the HDRB base-isolation system can be used for the structural model considered in this study.

The need for component-level verification is supported by recent structural-evaluation studies. Alrasyidi et al. (2026) emphasized that the bearing system controls the transfer of seismic force to the substructure, while Yudoprasetyo et al. (2025) showed that numerical structural evaluation should be complemented by component-capacity checks to confirm the adequacy of critical structural elements. In the present study, this principle is applied by checking the compressive-stress utilization ratio of each HDRB type rather than relying only on the global response reduction.

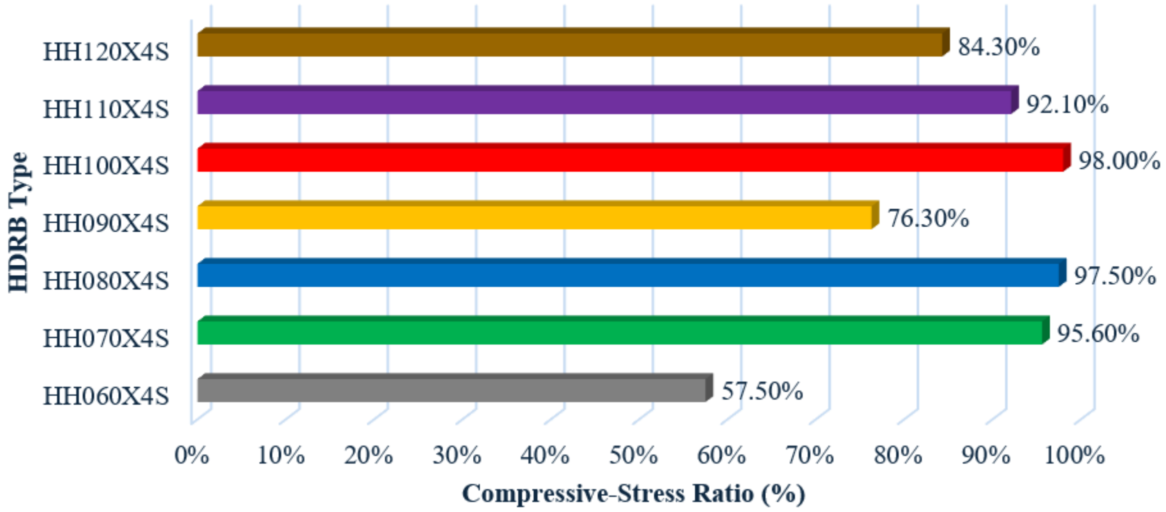

Figure 8. Compressive-stress utilization ratio of HDRB isolators

Comparison Between the Fixed-Base and HDRB Base-Isolation Models

The comparison between the fixed-base model and the HDRB base-isolation model shows that the use of HDRB produces significant changes in the dynamic response of the structure. The increase in structural period results in reduced base shear, while the drift control indicates a more controlled superstructure response. A summary of the structural-performance comparison is presented in Table 8.

Table 8. Summary of structural-performance comparison

Parameter	Fixed-base model	HDRB base-isolation model	Interpretation
X-direction period	2.425 s	4.758 s	HDRB lengthens the structural period.
Y-direction period	2.285 s	4.322 s	HDRB lengthens the structural period.
X-direction base shear	18,055.62 kN	9,580.43 kN	Reduction of 46.94%.
Y-direction base shear	18,088.09 kN	12,005.90 kN	Reduction of 33.63%.
Interstory drift control	Several stories exceed the allowable limit	All stories satisfy the allowable limit	HDRB improves drift control.
Lateral restoring force	-	41,673.708 kN >= 9,517.663 kN	The HDRB system satisfies the restoring-force control.
Compressive-stress control	-	$\sigma_{act,max}$ = 12.74 MPa < σ_{all} = 13.0 MPa	HDRB satisfies the compressive-stress control.

From the perspective of superstructure members, the reduction in internal forces in the HDRB model allows simplification or reduction of several beam and column members compared with the fixed-base model. The beam-type comparison is presented in Table 9, the column-type comparison is presented in Table 10, and the reinforcement-efficiency summary is presented in Table 11.

Table 9. Comparison of beam members between the fixed-base and HDRB base-isolation models

Fixed-base beam type	b (mm)	h (mm)	HDRB beam type	b (mm)	h (mm)
B57	500	700	B57	500	700
B58	500	800	B46	400	600
B59	500	900	B47	400	700
B510	500	1000	B49	400	900
B3A6	350	600	B3A6	350	600
B2A4	250	400	B2A4	250	400
B4A9	450	900	B57	500	700
B34	300	400	B3A6	350	600
B35	300	500	B3A6	350	600
B45	400	500	B46	400	600
B54	500	400	B46	400	600
B55	500	500	B46	400	600
B67	600	700	B47	400	700
B74	700	400	B47	400	700
B88	800	800	B47	400	700
B208	800	2000	B615	600	1500
B410	400	1000	B49	400	900
B610	600	1000	B49	400	900

The column comparison also shows a similar tendency. Several column types in the fixed-base model can be replaced by smaller dimensions in the HDRB model, for example K99 becomes K88, K1010 becomes K99, and K1111 becomes K1010. The comparison of column types is presented in Table 10.

To present the reinforcement comparison more efficiently for paper format, the detailed beam and column schedules are summarized using the number of representative member types, total bar count, and equivalent longitudinal steel-area index. The index was calculated as the sum of $n \times \pi d^2/4$ for the reinforcement entries listed in the comparison schedules; therefore, it reflects both the number of bars and the bar diameter.

As shown in Table 11, the HDRB model simplifies the representative beam schedule from 18 to 7 beam types and reduces the total longitudinal-bar count by 19.3%. For columns, the paired-column comparison shows a 15.7% reduction in main-bar count and a 41.6% reduction in equivalent main steel-area index. When the additional KP1515 column in the HDRB model is conservatively included, the column steel-area index is still 22.5% lower than the fixed-base schedule. These results support the interpretation that the reduction in seismic demand due to HDRB can lead to more efficient superstructure reinforcement, although final reinforcement design still depends on detailing requirements and element-specific strength checks.

Table 10. Comparison of column members between the fixed-base and HDRB base-isolation models

Fixed-base column type	b (mm)	h (mm)	HDRB column type	b (mm)	h (mm)
K66	600	600	K66	600	600
K67	600	700	K66	600	600
K77	700	700	K77	700	700
K88	800	800	K88	800	800
K99	900	900	K88	800	800
K1010	1000	1000	K99	900	900
K1011	1000	1100	K99	900	900
K1111	1100	1100	K1010	1000	1000
-	-	-	KP 1515	1500	1500

Table 11. Efficient summary of beam and column reinforcement comparison

Component	Metric	Fixed-base model	HDRB base-isolation model	Change indicated by HDRB
Beam flexural reinforcement	Representative beam types	18 types	7 types	61.1% fewer types
Beam flexural reinforcement	Longitudinal-bar count in the representative schedule	659 bars	532 bars	19.3% lower
Beam flexural reinforcement	Equivalent flexural steel-area index	249,461 mm²	243,728 mm²	2.3% lower
Column main reinforcement	Representative column types	8 types	6 types, including KP1515	25.0% fewer types
Column main reinforcement	Comparable main-bar count (paired columns only)	242 bars	204 bars	15.7% lower
Column main reinforcement	Comparable main steel-area index (paired columns only)	138,131 mm²	80,648 mm²	41.6% lower
Column main reinforcement	Conservative main steel-area index including KP1515	138,131 mm²	107,069 mm²	22.5% lower

This reinforcement-efficiency finding is also supported by Borneo Engineering studies on reinforced-concrete member design. Prasetya et al. (2021) showed that changes in design provisions and assumptions can affect the flexural and shear reinforcement requirements of structural beams. Hernadi et al. (2021) emphasized that column adequacy depends on axial-flexural interaction and strength-reduction factors. Therefore, the reduction in beam and column reinforcement in the HDRB model should be interpreted as a consequence of lower seismic demand; nevertheless, the final design must still satisfy element-level strength, detailing, ductility, and constructability requirements under SNI 2847:2019.

The discussion in this study focuses on the dynamic structural response, HDRB system behavior, and changes in the demand for superstructure members. Geotechnical evaluation, foundation design, soil bearing capacity, settlement, and soil-structure interaction are outside the scope of this study. The soft-soil site class SE is used only as a parameter for determining the seismic response spectrum at the Jakarta location.

Overall, HDRB base isolation is more effective than the fixed-base method for the lecture building in Jakarta because it reduces base shear, improves interstory drift control, and satisfies the lateral restoring-force and compressive-stress checks. Practical implementation still requires attention to isolator detailing, inspection access, and connection design between the superstructure, isolators, and substructure.

Conclusion

This study compared the fixed-base method and the High-Damping Rubber Bearing (HDRB) base-isolation method for an 11-story reinforced-concrete lecture building in Jakarta using response-spectrum analysis based on SNI 1726:2019. The results show that the use of HDRB substantially changes the dynamic characteristics of the structure by lengthening the fundamental period from 2.425 s to 4.758 s in the X direction and from 2.285 s to 4.322 s in the Y direction. This period shift confirms that the isolator provides horizontal flexibility at the base level, thereby reducing the seismic demand transmitted to the superstructure.

The HDRB base-isolation model reduces the seismic base shear from 18,055.62 kN to 9,580.43 kN in the X direction and from 18,088.09 kN to 12,005.90 kN in the Y direction, corresponding to reductions of 46.94% and 33.63%, respectively. The interstory-drift evaluation also indicates a more favorable response in the isolated model. Several stories in the fixed-base model exceed the allowable drift limit, whereas all stories in the HDRB model remain within the permitted limits in both directions.

The isolation system also satisfies the required safety checks. The lateral restoring force of 41,673.708 kN is greater than the minimum requirement of 0.025W, or 9,517.663 kN. The compressive-stress verification indicates that all HDRB types remain below their allowable stresses, with the most critical case occurring in the HH100X4S isolator, which reaches a utilization ratio of 98.01%. This result confirms that the selected HDRB configuration provides adequate restoring capacity and vertical-load stability for the structural model considered in this study.

From the perspective of superstructure design, the reduction in seismic demand contributes to a more efficient reinforcement arrangement. The representative beam schedule is simplified from 18 to 7 beam types, the longitudinal reinforcement count is reduced by 19.3%, and the comparable column main-steel area index decreases by 41.6%. Therefore, HDRB base isolation is effective not only in improving seismic response but also in supporting a more efficient reinforced-concrete design. This study is limited to structural response evaluation; geotechnical aspects, foundation capacity, settlement, soil-structure interaction, construction cost, and maintenance requirements were not evaluated. Future research should include nonlinear time-history analysis, comparisons with other isolator systems such as LRB and FPS, and life-cycle cost assessment to support practical implementation in Indonesian building projects.

Author Contributions

Conceptualization, M.S.M and K.Y.; Methodology, K.Y and R.B.A.A.; Software, R.H.; Validation, M.S.M and Y.N.W.; Formal Analysis, M.F.R.; Investigation, I.F.R.; Resources, R.B.A.A and I.F.R.; Data Curation, M.S.M and K.Y.; Writing – Original Draft Preparation, K.Y.; Writing – Review & Editing, M.S.M and K.Y.; Visualization, Y.N.W.; Supervision, R.B.A.A.; Project Administration, R.B.A.A and I.F.R.

Funding

No funding support was received

Conflicts of Interest

The all authors declare no conflict of interest.

Data Availability

The datasets generated during and/ or analyzedduring the current study are available from the corresponding author on reasonable request.

Use of Generative AI

No generative AI was used.

References

Alrasyidi, M. A., Rosyidi, M. F., Yudoprasetyo, K., & Munawaroh, P. Al. (2026). Analisis Pengaruh Lead Rubber Bearing Terhadap Kinerja Pilar Konvensional pada Struktur Jembatan Highway Ortotropik Dengan Non Linear. *Bangunan: Teori, Praktek, Penelitian, Dan Pengajaran Teknik Bangunan*, *31*(1), 1–12. https://doi.org/10.17977/um071v31i12026p1-12

Badan Standardisasi Nasional. (2019). Tata Cara Perencanaan Ketahanan Gempa Untuk Struktur Bangunan Gedung dan Non Gedung. In *Sni 1726:2019* (Issue 8, p. 254). Badan Standardisasi Nasional. http://akses-sispk.bsn.go.id//Upload/Dokumen/SK_SNI/SK_SNI_693_KEP_BSN_12_2019.pdf

Badan Standarisasi Nasional. (2020). *SNI 1727:2020 Beban desain minimum dan kriteria terkait untuk bangunan gedung dan struktur lain*. Badan Standarisasi Nasional.

Bridgestone Corporation. (2010). *High-Damping Rubber Bearings for Base Isolation*.

Computers & Structures, I. (2025). *CSI Analysis Reference Manual For SAP2000, ETABS, SAFE, and CSiBridge*. www.csiamerica.com

Fakrunnisa, I., & Hayu, G. (2022). Analisis Kinerja High Damping Rubber Bearing dan Lead Rubber Bearing pada Bangunan Beton Bertulang. *Jurnal Rekayasa Sipil Dan Lingkungan*, *5*, 48. https://doi.org/10.19184/jrsl.v5i1.23527

Firmansyah, M. F., Habieba, A. B., & Faimun, F. (2025). A Study on the Effects of Implementing Base Isolation System for Existing RC Buildings on Soft Soil. *Journal of Civil Engineering*, *40*(1 SE-), 12. https://doi.org/10.12962/j20861206.v40i1.7268

Grecia Istiqomah; Herman, Nanang Dalil, A. I. (2025). Comparison of Structural Performance of Fixbase and Base Isolation in KAI Boutique Hotel Building with Response Spectrum. *Portal: Jurnal Teknik Sipil*, *Vol 17*, *No 2 (2025): October Edition*, 87–91. https://doi.org/10.30811/portal.v17i2.7736

Hariyanto, I. R., Suswanto, B., & Habieb, A. B. (2022). Analisis Numerik Vertical Shear Link (VSL) secara Sub-Assemblage menggunakan Program Bantu ABAQUS. *Jurnal Aplikasi Teknik Sipil*, *20*(3), 333. https://doi.org/10.12962/j2579-891x.v20i3.13298

Hariyanto, I., Suswanto, B., Habieb, A. B., & Raka, I. G. P. (2025). Studi Analisis Perkuatan Struktur Gedung 5 Lantai Di Surabaya Akibat Beban Dinamis Menggunakan Shearwall. *Bangunan: Teori, Praktek, Penelitian, Dan Pengajaran Teknik Bangunan*, *30*(2), 153–168. https://doi.org/10.17977/um071v30i22025p153-168

Hariyanto Kohar; Wibowo, Yosi Noviari; Mansur, Moh. Safi'i; Rosyidi, Moh. Fadhlan; Fauzan, Irfan, I. R. Y. (2026). Evaluasi Strategi Retrofitting Seismik pada Bangunan Eksisting: Analisis Komparatif Sistem Isolasi Dasar dan Sistem Peredam pada Bangunan Bertingkat Menengah. *RIGGS: Journal of Artificial Intelligence and Digital Business*, *Vol. 5 No. 1 (2026): Februari-April*, 2913–2921. https://doi.org/10.31004/riggs.v5i1.6071

Hernadi, A. (2019). Analisis Spektrum Respon Gempa Menggunakan Peta Gempa SNI 1726 : 2002 , SNI 1726 : 2012 dan SNI 1726 : 2019 di Kota Tarakan. *Borneo Engineering : Jurnal Teknik Sipil*, *5*(3), 335–347. https://doi.org/https://doi.org/10.35334/be.v5i3.3579

Hernadi, A., Sahara, R., & Dewi, S. (2021). Perbandingan Kekuatan Kolom Berdasarkan SNI 2847:2013 dan SNI 2847:2019. *Borneo Engineering : Jurnal Teknik Sipil*, *5*, 237–247. https://doi.org/10.35334/be.v5i3.1661

Husen, M. F., Mentari, S., & Nursani, R. (2024). Comparative study of earthquake – resistant building design according to SNI 03-1726-2019 in Jakarta and Aceh regions. *IOP Conference Series: Earth and Environmental Science*, *1416*(1), 12006. https://doi.org/10.1088/1755-1315/1416/1/012006

Istiono, H., & Lisawiyani, Y. (2022). Studi Komparasi Perilaku Struktur Gedung At-Tauhid Di Kota Surabaya Dengan Menggunakan SNI 1726-2012 Dan SNI 1726-2019. *Borneo Engineering : Jurnal Teknik Sipil*, *1*, 11–20. https://doi.org/10.35334/be.v1i1.1854

Masaki, N., Mori, T., Murota, N., & Kasai, K. (2016). *Validation of Hysteresis Model of Deformation-History Integral Type for High Damping Rubber Bearings*. https://api.semanticscholar.org/CorpusID:211052964

Maulida, A., Umniati, B. S., Sulton, M., & Maulidani, A. (2025). Performance Based Design: Performance Analysis on Fixed Base Structure and Structures with High Damping Rubber Bearing. *BENTANG Jurnal Teoritis Dan Terapan Bidang Rekayasa Sipil*, *13*, 11–22. https://doi.org/10.33558/bentang.v13i1.10112

Munthe M, A. T. I. (2020). Comparative Study Of Structure Response Isolated Base And Not Isolated Base on IHF School Cimanggis. *Journal of World Conference (JWC)*, *Vol. 2 No. 2 (2020): March 2020*, 106–118. http://proceedings.worldconference.id/index.php/prd/article/view/205/92

Oh, J., Kim, J., & Han, S. (2017). An experimental study on the shear property dependency of high-damping rubber bearings. *Journal of Vibroengineering*, *19*. https://doi.org/10.21595/jve.2017.18652

Park, K., Mazda, T., & Kajita, Y. (2023). Research on Hysteresis Model of High Damping Rubber Bearings Considering Mechanical Properties Based on Dynamic Loading Test. In *Proceedings of 5th International Conference on Civil Engineering and Architecture* (pp. 1069–1080). https://doi.org/10.1007/978-981-99-4049-3_82

Patel, D., Kumar, R., Mourya, V., & Pandey, G. (2024). Dynamic behavior of high damping rubber bearings and lead rubber bearings under near-fault earthquakes. *Research on Engineering Structures and Materials*. https://doi.org/10.17515/resm2024.194ea0225rs

Prasetya, N., Hernadi, A., & Nugroho, A. (2021). Studi Komparasi Perancangan Balok Struktural Berdasarkan SNI 2847-2002, SNI 2847-2013 Dan SNI 2847-2019. *Borneo Engineering : Jurnal Teknik Sipil*, *5*, 294–306. https://doi.org/10.35334/be.v5i3.1874

Rahardjo, I. P., Tajunnisa, Y., Komara, I., Arifa, G. N., Sungkono, & Wahyudi, D. I. (2023). Performance of High-Damping Rubber Bearings for Seismic Isolation – Case Study of Nayumi Sam Tower Malang Apartment. *IPTEK The Journal of Engineering*, *9*(3 SE-Articles), 106–110. https://journal.its.ac.id/index.php/joe/article/view/8194

Rayendra, M., & Tavio. (2024). Effect of High-Damping Rubber Bearings on Performance of High-Rise Buildings in Highly and Moderate Seismic Regions BT - Advances in Civil Engineering Materials. In E. M. Nia & M. Awang (Eds.), *Advances in Civil Engineering Materials* (pp. 177–187). Springer Nature Singapore.

Santoso, A., & Saito, T. (2024). An Investigation of Dynamic Soil-Structure Interaction on the Seismic Behavior of RC Base-Isolated Buildings. *Civil Engineering Journal*, *10*, 3455–3472.

https://doi.org/10.28991/CEJ-2024-010-11-01

Shahabi, A., Ahari, G., & Barghian, M. (2020). Base Isolation Systems – A State of the Art Review According to Their Mechanism. *Journal of Rehabilitation in Civil Engineering*, *8*(2). https://doi.org/10.22075/jrce.2019.16186.1306

Suwondo, R., Susanto, D., Suangga, M., & Alama, M. S. (2025). Earthquake Resilience in Low-Rise Concrete Buildings: A Study on the Effectiveness of Base Isolators. *International Journal on Advanced Science, Engineering and Information Technology*, *15*(2 SE-Articles), 633–639. https://doi.org/10.18517/ijaseit.15.2.20636

Wibowo, H. A., Meilano, I., & Virtriana, R. (2024). Assessing Potential Earthquake-Induced Structural Damage and Losses in School Buildings, West Java, Indonesia. *Papers in Applied Geography*, *10*(2), 138–153. https://doi.org/10.1080/23754931.2024.2323719

Yudoprasetyo, K., Prasetya, A. D., Rosyidi, M. F., Hariyanto, R., Wibowo, Y. N., Anugraha, R. B., Safi, M., Ashara, K. F., & Sigit, M. (2025). Upaya Penguatan Keselamatan Prasarana Sekolah melalui Evaluasi Teknis Struktur Kolom pada Bangunan Pendidikan di Bojonegoro. *Inovasi Jurnal Pengabdian Masyarakat*, *3*(3), 255–266. https://doi.org/10.54082/ijpm.1063